

Antioxidant, antiglycation, and antibacterial of copper oxide nanoparticles synthesized using *Caesalpinia Sappan* extract

Mathurada Sasarom^{1,2}, Phenphichar Wanachantararak³, Pisaisit Chaijareenont^{4,5}, Siriporn Okonogi^{2,5,*}

¹ PhD Degree Program in Pharmacy, Faculty of Pharmacy, Chiang Mai University, Chiang Mai, Thailand

² Department of Pharmaceutical Sciences, Faculty of Pharmacy, Chiang Mai University, Chiang Mai, Thailand;

³ Dentistry Research Center, Faculty of Dentistry, Chiang Mai University, Chiang Mai, Thailand;

⁴ Department of Prosthodontics, Faculty of Dentistry, Chiang Mai University, Chiang Mai, Thailand;

⁵ Center of Excellence in Pharmaceutical Nanotechnology, Faculty of Pharmacy, Chiang Mai University, Chiang Mai, Thailand.

SUMMARY Synthesis of metal nanoparticles using plant extracts is environmentally friendly and of increasing interest. However, not all plant extracts can meet successfully on the synthesis. Therefore, searching for the high potential extracts that can reduce the metal salt precursor in the synthesis reaction is essential. The present study explores the synthesis of copper oxide nanoparticles (CuONPs) using *Caesalpinia sappan* heartwood extract. Phytochemical analysis and determination of the total phenolic content of the extract were performed before use as a reducing agent. Under the suitable synthesized condition, a color change in the color of the solutions to brown confirmed the formation of CuONPs. The obtained CuONPs were confirmed using ultraviolet-visible spectroscopy, photon correlation spectroscopy, X-ray diffraction, scanning electron microscope, energy dispersive X-ray, and Fourier transform infrared analysis. The synthesized CuONPs investigated for antioxidant, antiglycation, and antibacterial activities. CuONPs possessed antioxidant activities by quenching free radicals with an IC₅₀ value of 63.35 µg/mL and reducing activity with an EC range of 3.19-10.27 mM/mg. CuONPs also inhibited the formation of advanced glycation end products in the bovine serum albumin/ribose model with an IC₅₀ value of 17.05 µg/mL. In addition, CuONPs showed inhibition of human pathogens, including Gram-positive *Staphylococcus aureus* and Gram-negative *Escherichia coli*, and prevention of biofilm formation and biofilm eradication, with maximum inhibition of approx. 75%. Our findings suggest that *C. sappan* extract can be used to obtain highly bioactive CuONPs for the development of certain medical devices and therapeutic agents.

Keywords *Caesalpinia Sappan*, copper oxide nanoparticles, antioxidant activity, antiglycation activity, antibacterial activity

1. Introduction

Nanotechnology is an emerging field of science that are received attention in many fields such as pharmaceutical (1), food industry (2), electronics and energy, mechanics and space industries (3). Nanomaterials exhibit activities which are different from bulk materials due to their nano size, surface, high surface to volume ratio and aggregation properties and biological properties (4). Metal and metal oxide nanoparticles are emerging as potential candidates in the field of nanoscience and nanotechnology. Metal oxide nanoparticles such as ferric oxide, zinc oxide, titanium oxide, and copper oxide have been investigated for their environmental and biomedical applications (5). Among them, copper

oxide nanoparticles (CuONPs) have gained the great interest due to low cost for synthesis, their widespread application in electronic, optical sensors, catalysts and therapeutic applications (6).

The synthesis of metal nanoparticles can be achieved through two ways, physical and chemical methods. The physical methods consume high physical energy, such as high temperature and high pressure. This may have an economic impact on production. In chemical methods, harmful chemicals are often used as a reducing to convert metal salt to metal nanoparticles. These hazardous chemicals are not environmentally friendly. Biosynthesis is the most suitable alternative method for producing metal nanoparticles because it is non-toxic and cost-effective. In the process of

biosynthesis, environmentally friendly agents including biological components from plants and biometabolites from organisms such as bacteria, algae and fungus are used instead of hazardous chemicals (7). Therefore, biosynthesis is often referred to as green synthesis. Among the natural reducing agents, plant extracts have been attracted the interest for the synthesis because the plant bioactive components can act not only as a reducing agent but also often act as a stabilizing agent by preventing aggregation of the nanoparticles (8). There are some reports on using plant extracts in biosynthesis of CuONPs (9–11). However, the obtained information is still less compared to the vast number of plant species. Therefore, it is interesting to search for other new potential plants to obtain CuONPs with several biological activities.

Caesalpinia sappan (Leguminosae) is distributed in southeast Asia. It has been used as a food coloring and for medicinal purposes from ancient times to the present. The heartwood of *C. sappan* was reported to have antioxidant activity (12) and has been used in Thai folk medicine for treatment of many diseases and disorders such as tuberculosis, diarrhea, skin infections and bleeding (13). *C. sappan* extract was previously used for biosynthesis of silver nanoparticles (14). Our group has developed CuONPs using *C. sappan* extract and reported that pH of the reaction affected the resulting nanoparticles. We also reported that the most optimum pH yielded the CuONPs with good characteristics and high antifungal activity against *C. albicans* (15). In the present study, CuONPs were synthesized at the optimum pH using the aqueous extract of *C. sappan* as a reducing agent. The obtained CuONPs were evaluated for antioxidant, antiglycation, antibacterial and antibiofilm activity against Gram positive and Gram-negative bacteria. In addition, the stabilizing effect of the extract on the obtained nanoparticles was also observed.

2. Materials and Methods

2.1. Materials

Ferric chloride, potassium persulfate, 2, 2'-azinobis-(3-ethylbenzothiazoline-6-sulfonate) (ABTS), ribose, methylglyoxal (MGO), and aminoguanidine were from Sigma-Aldrich (MO, USA). Copper sulfate, hydrochloric acid (HCl) and phosphate buffer solution (PBS) were from Merck (Darmstadt, Germany). Ascorbic acid and Fe³⁺-2, 4, 6-tripyridyl-S-triazine (TPTZ) were from Fluka Chemicals (Buchs, Switzerland). Bovine serum albumin (BSA) were purchased from Himedia Labs (Mumbai, India). Sodium carbonate, aluminum chloride and sodium hydroxide were from RCI Labscan (Bangkok, Thailand). Tryptic soy broth (TSB) and Tryptic soy agar (TSA) were purchased from Difco (Maryland, USA). Ampicillin was

from Serva (Heidelberg, Germany). Other chemicals and solvents are analytical grade.

2.2. Preparation of the extract

The heartwood of *C. sappan*, purchased from the local market in Chiang Mai, Thailand, was washed with clean water, cut into small pieces, and dried at 50°C. The dried samples were ground into fine powder. *C. sappan* extract was prepared by adding 5.0 g of the plant powder into 50 mL distilled water. The mixture was stirred at 500 rpm overnight and then filtered through a Whatman filter paper. The obtained filtrate was centrifuged at 3000×g for 10 min to eliminate some tiny precipitations and subsequently lyophilized using a freeze dryer (Christ Beta 2-8 LD plus, Osterode am Harz, Germany). The resulting dried powder was stored in the refrigerator until use.

2.3. Phytochemical analysis and determination of total phenolic content

The presence of various phytochemical constituents such as tannins, saponins, alkaloids, flavonoids and terpenoids in *C. sappan* extract was performed based on the standard procedure (16). Briefly, each 20 mg/mL of the extract was subjected to identify the presence of tannins using ferric chloride test, saponins using frothing test, alkaloids using Dragendorff reagent, flavonoids using Shibita's reaction test, and terpenoids using Salkowski test. These tests are qualitative and are based on discoloration, foaming, or sedimentation. It depends on the phytochemicals in the extract and the specific chemical reagents.

The total phenolic content of the samples was determined by Folin-Ciocalteu method previously described (17) with some modifications. Briefly, 20 µL of 10 mg/mL of the extract was mixed with 45 µL of Folin-Ciocalteu reagent and incubated for 3 min at room temperature. Next, 135 µL of 25% (w/v) sodium carbonate solution was added to the mixture and incubated at in the dark room temperature for 1 h. The absorbance of the mixture was measured at 750 nm using a microplate reader (Spectrostar Nano, BMG Labtech, Ortenberg, Germany). Results were expressed as mg of gallic acid equivalent (GAE) per µg of samples.

2.4. Biosynthesis of CuONPs

In the process of CuONPs biosynthesis, copper sulfate was used as a precursor and the aqueous extract of *C. sappan* was used as a reducing agent. An exact volume of 19 mL of 10 mM copper sulfate solution was heated at 70°C. Then, 1 mL of *C. sappan* extract solution was added with constant stirring for 30 min. Next, 1 M sodium hydroxide was added until the mixture reached pH 10. Afterward, the mixture was continually reacted

at 70°C for 2 h or until the color of the mixture was obviously changed. The mixture was washed with Milli-Q water by centrifugation at 8000× *g* for 30 min (three times). The resulting precipitate was dispersed in absolute ethanol and dried at 60°C for 8 h.

2.5. Characterization of CuONPs

The absorbance of CuONPs in the range 200 to 800 nm was measured using a UV-Vis spectrophotometer (UV-2450, Shimadzu, Kyoto, Japan). An aliquot of 10 mg/mL of CuONPs in Milli-Q water was diluted 10 times and subjected to sonication prior to the measurements. The Milli-Q water was used as a blank. To investigate the functional groups presenting in the extract and the surface of CuONPs, the spectra of the samples collected from Fourier-transform infrared spectroscopy (FTIR) was analyzed using FTIR (Thermo Nicolet/470FT-IR spectrometer, Nicolet Nexus, Madison, USA) at a resolution of 32 cm⁻¹ in the range of 4,000 to 500 cm⁻¹. The particle size, size distribution expressed as a polydispersity index (PDI), and zeta potential of CuONPs were determined by dynamic light scattering (DLS) method using a Malvern Zetasizer Nano ZS (Malvern Instruments Company, Worcestershire, UK). To prepare a sample for DLS, 1 mg/mL of CuONPs in Milli-Q water was diluted 10 times and subjected to sonication prior to the measurements. The hydrodynamic size and size distribution of the CuONPs was measured at a fixed angle of 173°. The zeta potential of CuONPs was automatically calculated based on the Smoluchowski equation using the Zetasizer (Malvern Instruments Company) software version 7.1. All experiments were performed in triplicate. The surface morphology and elemental composition of CuONPs were verified by field-emission scanning electron microscopy (SEM) equipped with an energy dispersive X-ray (EDX) analysis system using SEM Microscope (JSM 6335 F, JEOL Ltd, Tokyo, Japan). The crystalline characteristics of the samples were evaluated by X-ray diffraction (XRD) pattern using a diffractometer (Rigaku SmartLab, Tokyo, Japan) in the 2θ range of 20°-80°.

2.6. Determination of antioxidant assays

2.6.1. ABTS radical scavenging assay

The scavenging activity of ABTS radicals of the samples was carried out according to the method previously described (18) with some modifications. Briefly, free radicals of ABTS were generated by oxidizing 7 mM ABTS with 2.45 mM potassium persulfate. The mixture was incubated for 16-18 h in the dark at room temperature. The ABTS radical solution was diluted with deionized water to adjust the absorbance of 0.7 ± 0.2 at 750 nm. Then, 20 μL of the samples at various concentrations was treated with 180 μL of the radical

solution. The samples were allowed to stand in a dark environment for 30 min and measured the absorbance at 750 nm using a microplate reader (Spectrostar Nano). Ascorbic acid was used as a positive control. The scavenging activity of ABTS radicals was expressed as the percentage of inhibition, which was calculated using the following equation: PI (%) = [(A_C-A_S)/A_C] × 100.

Where PI is the percentage of inhibition, A_C is the absorbance of control (containing all reagents except the sample or the positive control) and A_S is the absorption of the samples. The result was expressed as the concentration of sample required for inhibition of 50% of ABTS radicals (IC₅₀ value).

2.6.2. Ferric reducing antioxidant power (FRAP)

The reducing activity of the samples was carried out according to the method previously described (17) with some modifications. Briefly, FRAP solution was freshly prepared by mixing 10 mM TPTZ in 40 mM hydrochloric acid, 20 mM ferric chloride, and 0.3 M acetate buffer (pH 3.6) in a volume ratio of 1:1:10. Then, an exact volume of 20 μL of the sample was added with 180 μL of the FRAP solution. After 30 min of mixing, the absorbance of the mixture was recorded at 595 nm using a microtiter plate reader (Spectrostar Nano). A standard curve was generated using FeSO₄ solution in the range of 0-2.5 mM. The reducing power of the sample was expressed as an equivalent capacity (EC) which was the ability to reduce ferric ions to ferrous ions, expressed as mM ferrous sulfate equivalents per milligram of the sample.

2.7. Antiglycation

2.7.1. BSA-ribose glycation model

The glycation of BSA was performed according to the methods previously described (19,20) with some modifications. Briefly, 200 μL of 50 mg/mL BSA was mixed with 400 μL of 1.25 M ribose containing 0.02% sodium azide. Besides, 200 μL of 50 mg/mL BSA in PBS, pH 7.4 without ribose solution was used as a blank control. Then, 100 μL of each sample was added to the mixture with or without ribose. All mixtures were adjusted to a final volume of 1 mL with 0.1M PBS, pH 7.4. All reaction mixtures were incubated in the dark at 45°C for 3 days. After 3 days incubation, 200μL of the reaction mixture was dispensed into the wells of a 96-well black micro-plate to measure the formation of advanced glycation end products (AGE) using fluorescent intensity at an excitation wavelength of 370 nm and an emission wavelength of 440 nm by a microplate reader (SpectraMax M3, Molecular devices, California, USA). The percentage of AGE inhibition was calculated using the following equation: PAI (%) = [(F_C-F_{CB})-(F_S-F_{SB})]/(F_C-F_{CB}) × 100.

Where PAI was the percentage inhibition of AGE, F_C and F_{CB} were the fluorescent intensity of the control with ribose and the blank control without ribose, respectively. F_S and F_{SB} were the fluorescent intensity of sample with ribose and blank of sample without ribose, respectively. The 50% AGE inhibition (IC_{50} value) was calculated from PAI of various concentrations of the samples.

2.7.2. BSA-MGO glycation model

The evaluation for the inhibition of the middle stage of the protein was performed according to the method previously described (21) with some modifications. Briefly, 200 μ L of 50 mg/mL BSA was mixed with 50 μ L of 300 mM MGO. Besides, 200 μ L of 50 mg/mL BSA in PBS, pH 7.4 was used as a blank control. Then, 100 μ L of each sample was added to the mixture with or without MGO. The mixtures were adjusted to a final volume of 1 mL with 0.1M PBS, pH 7.4. All reaction mixture was incubated in the dark at 45°C for 7 days. After 7 days incubation, the formation of AGE was determined and calculated using the same condition and equation as a BSA-ribose model.

2.8. Antibacterial activity

In this study, *Staphylococcus aureus* DMST 8013 and *Escherichia coli* DMST 15537 were used as human pathogenic Gram-positive and Gram-negative bacteria, respectively. The bacterial strains were cultured in TSB and incubated at 37°C for 16 h prior to use. The suspension of these pathogenic strains was prepared and adjusted to the turbidity of 0.5 McFarland standard using a McFarland densitometer (DEN-1 Biosan, Riga, Latvia). Ampicillin was used as a positive control whereas the well without the samples was used as a negative control.

2.8.1. Determination of inhibition zone

The inhibition zone of samples to inhibit bacterial growth was determined using an agar well diffusion method. The suspension of each strain after adjusting to 0.5 McFarland standard was diluted to 1.5×10^6 colony forming unit (CFU)/mL. The agar plates were swabbed with bacterial suspension. A sterile cork-borer was used to prepare 5 mm-diameter wells in the petri dishes. An exact volume of 20 μ L of 10 mg/mL samples was dropped into each well. The plates were incubated in aerobic condition at 37°C for 16-18 h. After the incubation, the diameter of the clear zone indicating complete inhibition was measured. The experiment was performed in triplicate.

2.8.2. Determination of minimum inhibitory concentration (MIC) and minimum bactericidal concentration (MBC)

The determination of MIC and MBC of the samples

was carried out using a modified broth dilution method previously described (22) with some modifications. Briefly, the samples at a final concentration range from 0.016-4 mg/mL were dispersed in the 96-well microplates. Subsequently, 100 μ L of each strain suspension at 1.5×10^5 CFU/mL was added into the wells. The plates were then incubated at 37°C for 24 h. The lowest concentration that inhibited the visible growth of bacteria was considered as the MIC. To determine MBC, the cultures were further investigated by streaking on TSA agar plates. The agar plates were incubated at 37°C for 24 h. The lowest sample concentration in the plates where bacterial growth could not be visible was considered as the MBC. All experiments were performed in triplicate.

2.8.3. Antibiofilm activity

In this experiment, two mechanisms of antibiofilm activity of the samples; inhibition of biofilm formation and eradication of the formed biofilms were investigated using a method previously described (23) with some modifications. For the study of inhibition of bacterial biofilm formation, 100 μ L of each stain at 1×10^6 CFU/mL and 100 μ L of the samples at the final concentrations of 1/4 MIC, 1/2 MIC and MIC were added into 96-well plates. The plates were then incubated at 37°C for 24 h. For the biofilm eradication effect of the samples, 100 μ L of each stain at 1×10^6 CFU/mL and 100 μ L of TSB were transferred to 96-well plates and incubated at 37°C for 24 h for biofilm formation.

After incubation, the culture supernatants and planktonic cells in each well were discarded and washed with PBS three times to remove nonadherent planktonic cells. The resulting biofilms were stained with 200 μ L of 0.1% (w/v) crystal violet in the plates at room temperature for 30 min. The excess staining was removed by gently washing with 100 μ L of PBS. To determine adherence biofilms, the stained biofilms were solubilized with 100 μ L of 30% acetic acid for 15 min. The optical density of the stained biofilms solution was quantified by measuring at 595 nm using a microliter plate reader (Model 680, Bio-Rad, California, USA). All experiments were done in triplicate. The percentage of biofilm forming inhibition or biofilm eradication was calculated by the following equation: BFI (%) or BE (%) = $1 - (OD_s/OD_c) \times 100$. Where BFI or BE was the percentage of biofilm forming inhibition or biofilm eradication, OD_s and OD_c were the optical density of the sample and the control, respectively.

2.9. Statistical analysis

The results were expressed as mean \pm S.D. Statistical analysis was performed on SPSS software version 20 for Windows. Differences between groups were determined by one-way analysis of variance (ANOVA) followed by

Ducan's post hoc test. A p -value < 0.05 was considered statistically significant.

3. Results

3.1. Phytochemical study and total phenol content of *C. sappan*

The aqueous extract of *C. sappan* was subjected to the determination of phytochemicals. In the tannin test, dark green precipitates in the extract were observed. This result suggested the presence of tannins in the extract. The persistent froth of the extract was observed. This indicated the presence of saponins. In Shibta's reaction test, after adding some concentrated hydrochloric acid and a few magnesium filings, color changed from orange to pale red in the extract. This result confirmed the presence of flavonoids in the extract. In Salkowski test, the extract did not show any color change for terpenoids suggesting that there were no terpenoids in the extract. In Folin-Ciocalteu phenol assay, the result indicates that the total phenolic content of the aqueous extract of *C. sappan* was found to be 62.06 ± 3.13 mg GAE/g.

3.2. Preparation and characterization of the synthesized CuONPs.

In the preparation process, the color of the solution changed from colorless (of copper sulfate solution) and red color (of *C. sappan* extract) to brown as shown in Figure 1. The brown formation color indicated a complete reaction of biosynthesis. As this preparation was green synthesis, therefore the resulting CuONPs obtained were called green-CuONPs or G-CuONPs. The absorbance of G-CuONPs was found at 255 nm.

Using the Folin-Ciocalteu phenol assay, the result indicates that the total phenolic content of G-CuONPs was found to be 21.59 ± 1.28 mg GAE/g. The FTIR spectra of the aqueous extract of *C. sappan* and G-CuONPs are illustrated in Figure 2. The FT-IR

spectrum of the extract showed peaks around 3,400, 1,619, 1,505, 1,443, 1,317, and 663 cm^{-1} . The FT-IR spectrum of the extract showed a broad peak around 3,400 cm^{-1} which are assigned to OH stretching. Some other peaks at around 1,619, 1,505 and 1,443 cm^{-1} correspond to O-H, N-H, and carboxylate functional groups, respectively. Two other peaks at 1,317 and 663 cm^{-1} are due to the presence of C=O stretching vibration and C-H stretching (24). The FTIR spectrum of G-CuONPs shows the bands at 3,856, 1,547, and 528 cm^{-1} . The FTIR spectrum of G-CuONPs shows the bands at 3,856 and a broad peak at 1,547 cm^{-1} which represented the functional groups of the extract. Additionally, the peak at approximately 528 cm^{-1} was considered to be the characteristic band of cupric oxide (25).

Size, size distribution, and the zeta potential peak images of G-CuONPs are represented in Figure 3 (a) and (b). The average particle size of G-CuONPs was 296 ± 7 nm with a Pdl value of 0.340 ± 0.018 . The zeta potential of G-CuONPs is -30.03 ± 0.40 mV. The SEM image as shown in Figure 3 (c) revealed that G-CuONPs were small size with a spherical shape. The EDX of G-CuONPs shows the dominance of copper and oxygen as shown in Figure 3 (d), confirming that the synthesized nanoparticles were copper oxide. The XRD diffraction pattern of G-CuONPs indicates the identical crystalline peaks at 2θ of 22.85, 28.00, 30.45, 33.27, 35.72, 37.91, 41.28, 52.67, and 60.03°.

3.3. Antioxidant activity

In vitro antioxidant activity of *C. sappan* extract, copper sulfate, the synthesized G-CuONPs, and ascorbic acid was analyzed using ABTS free radical scavenging and FRAP assays. The results of free radical scavenging activity and IC_{50} of the samples are shown in Figure 4. It was found that G-CuONPs at a concentration range of 12.5-200 $\mu\text{g/mL}$ possess scavenging activity ranging from 19.78 ± 0.82 to $98.64 \pm 0.41\%$. The scavenging property of the aqueous extract of *C. sappan* at a

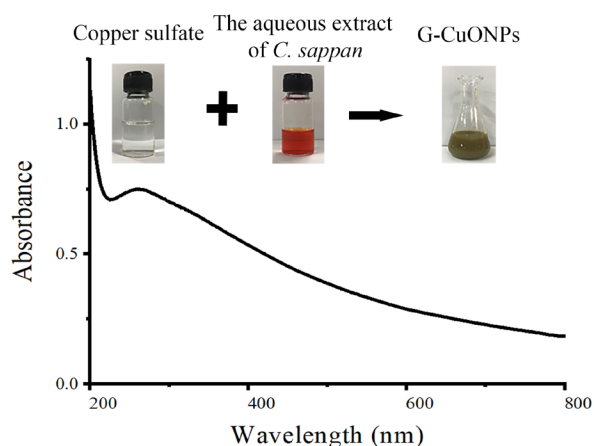


Figure 1. Photograph and UV-Visible spectrum of G-CuONPs.

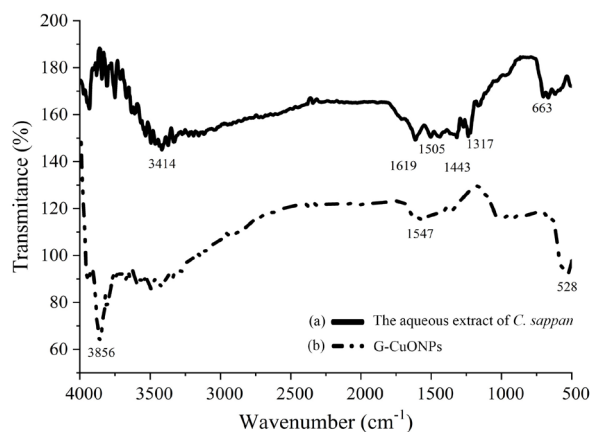


Figure 2. FT-IR spectra of (a) the aqueous extract of *C. sappan* and (b) G-CuONPs.

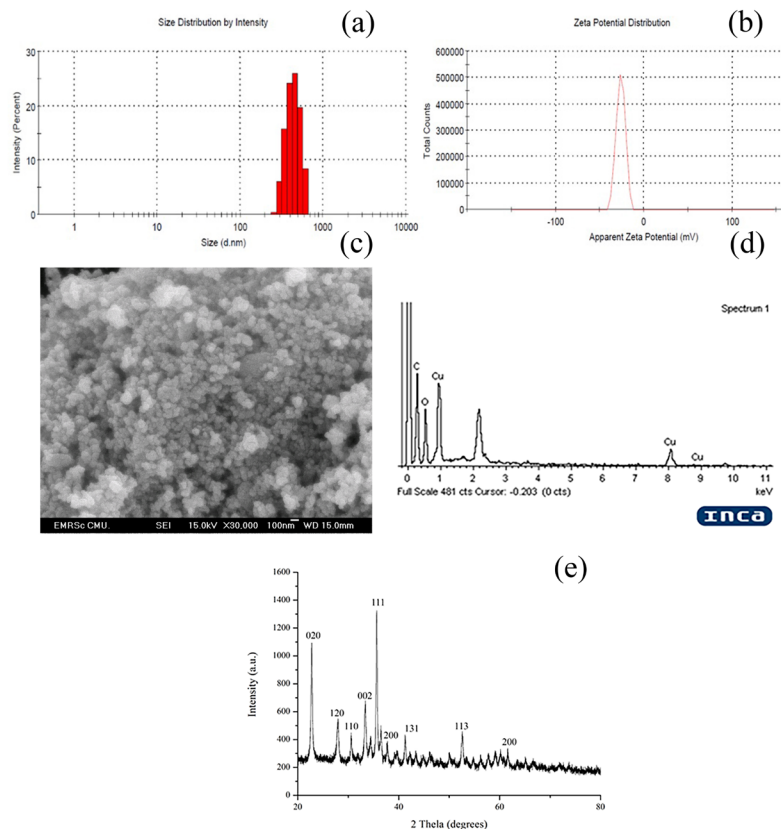


Figure 3. Size distribution (a), zeta potential (b), SEM (c), and EDX (d), and XRD analysis (e) of G-CuONPs.

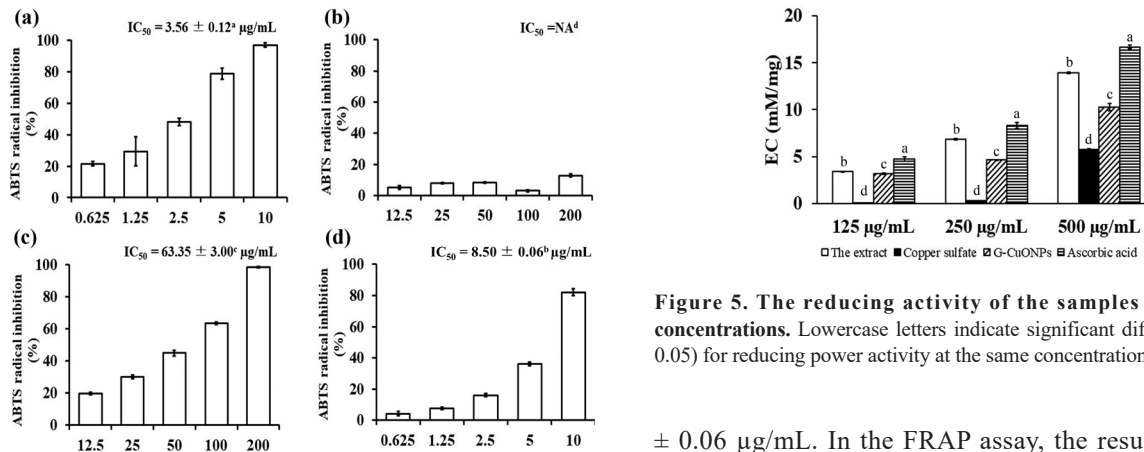


Figure 4. The radical scavenging activity of the aqueous extract of *C. sappan* (a), copper sulfate (b), G-CuONPs (c) and ascorbic acid (d). Lowercase letters above IC_{50} values indicate significant difference ($P < 0.05$) for each activity.

concentration range of 0.625-10 $\mu\text{g/mL}$ was found to be 21.53 ± 9.33 to 96.78 ± 1.39 %. Ascorbic acid, used as a positive control, at a concentration range of 0.625-10 $\mu\text{g/mL}$ shows 4.23 to 82.07 %. It is noted that the scavenging ability of all samples was dose-dependent manner. The IC_{50} values for radical scavenging of G-CuONPs and *C. sappan* extract were 63.35 ± 3.00 and 3.56 ± 0.12 $\mu\text{g/mL}$, respectively, while that of ascorbic acid was 8.50

Figure 5. The reducing activity of the samples at various concentrations. Lowercase letters indicate significant difference ($P < 0.05$) for reducing power activity at the same concentration of samples.

± 0.06 $\mu\text{g/mL}$. In the FRAP assay, the result showed that the reducing activities of all samples were dose-dependent manner as seen in Figure 5. It is found that G-CuONPs possess moderate reducing property, which is significantly higher than copper sulfate but less than *C. sappan* extract and ascorbic acid.

3.4. Antiglycation activity

In this experiment, BSA was used as a model protein to investigate AGE formation by fluorophoric AGE at λ excitation/emission 370/440 nm. Previous studies have reported the wide application of these excitation/emission wavelengths in determining AGE formation *in vitro* and *in vivo* (26,27). The results show that the AGE

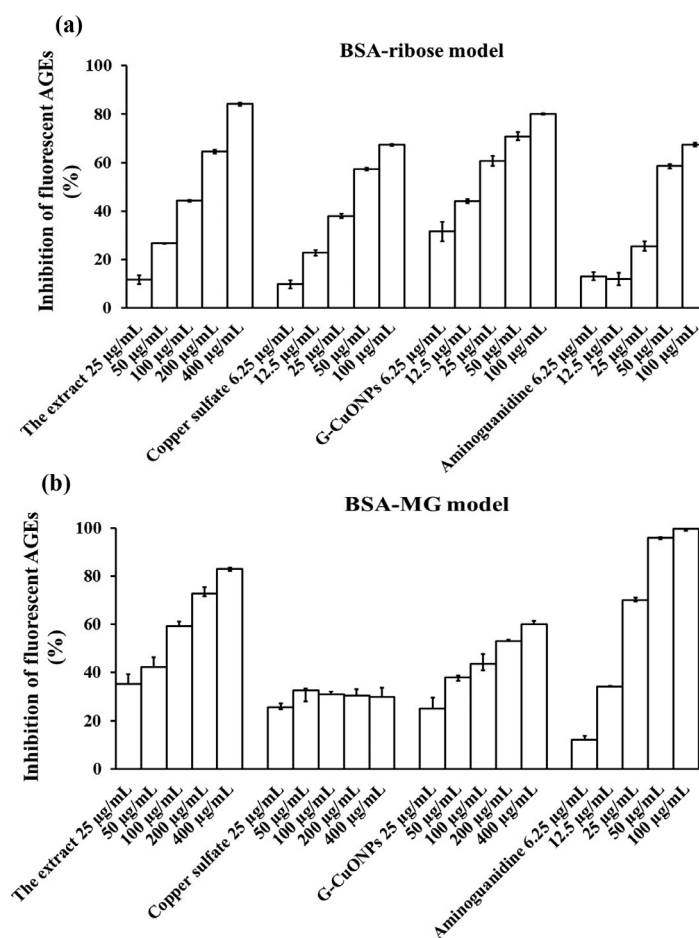


Figure 6. The antiglycation activity of the samples studied using BSA-ribose (a) and BSA-MGO (b) models.

inhibition effect of the samples varied depending on the glycation models. In BSA-ribose model, copper sulfate showed the AGE inhibition from 9.78 ± 1.67 to $67.36 \pm 0.35\%$ and G-CuONPs showed the inhibitory effect from 31.52 ± 4.08 to $80.14 \pm 0.33\%$. The positive control, aminoguanidine, had the inhibitory effect from 13.07 ± 1.75 to $67.37 \pm 0.83\%$ at the same concentration of 6.25-100 $\mu\text{g/mL}$ as shown in Figure 6 (a). The inhibition effect of *C. sappan* extract at a concentration range of 25-400 $\mu\text{g/mL}$ was 11.72 ± 1.83 to $84.23 \pm 0.64\%$. The results showed that G-CuONPs have the highest AGE inhibition effect with the lowest IC_{50} value of $17.05 \pm 0.92 \mu\text{g/mL}$ as shown in Table 1. From this result, copper sulfate showed moderate effect with IC_{50} value of $40.50 \pm 0.69 \mu\text{g/mL}$. Whereas the aqueous extract of *C. sappan* has the lowest effect with IC_{50} $191.15 \pm 31.73 \mu\text{g/mL}$. The low values of IC_{50} reflect the greater potency for the antiglycation activity of samples. In BSA-MG model, methylglyoxal is one of dicarbonyl species during AGE formation and can lead to cellular dysfunction and chronic diabetic complications (28). The samples exhibited different inhibition effects. The aqueous extract of *C. sappan* and G-CuONPs at the same concentrations at 25-400 $\mu\text{g/mL}$ showed AGE inhibition effect from 9.78 ± 1.67 to $67.36 \pm 0.35\%$ and 24.97 ± 4.59

Table 1. The IC_{50} values of the samples on inhibition of AGEs formation

Samples	IC_{50} ($\mu\text{g/mL}$)	
	Ribose	Methylglyoxal
<i>C. sappan</i> extract	$191.15 \pm 31.73^{\text{d}}$	$100.52 \pm 11.62^{\text{b}}$
Copper sulfate	$40.50 \pm 0.69^{\text{b}}$	$> 400^{\text{d}}$
G-CuONPs	$17.05 \pm 0.92^{\text{a}}$	$179.33 \pm 9.06^{\text{c}}$
Aminoguanidine	$33.39 \pm 0.06^{\text{c}}$	$18.44 \pm 2.02^{\text{a}}$

Lowercase letters indicate significantly different ($P < 0.05$) for antiglycation activity in each model.

to $60.12 \pm 1.15\%$, respectively, as shown in Figure 6 (b). Aminoguanidine, a positive control, at a concentration range of 6.25-100 $\mu\text{g/mL}$ shows the inhibition effect from 12.05 ± 1.58 to $99.62 \pm 0.71\%$. However, copper sulfate shows concentration independent effect. In this model, *C. sappan* extract exhibited higher effect than G-CuONPs. In addition, the inhibitory effects of *C. sappan* extract and G-CuONPs were lower than aminoguanidine.

3.5 Antibacterial activity

The result of this study demonstrated that *C. sappan* extract, copper sulfate, and G-CuONPs possessed

Table 2. Inhibition zone (IZ), minimum inhibition concentration (MIC) and minimum bactericidal concentration (MBC) of the samples against *E. coli* and *S. aureus*

Samples	<i>E. coli</i>			<i>S. aureus</i>		
	IZ (mm)	MIC*	MBC*	IZ (mm)	MIC*	MBC*
<i>C. sappan</i> extract	7 ± 0 ^c	2.0	2.0	7 ± 1 ^d	1.0	1.0
Copper sulfate	13 ± 2 ^b	1.0	2.0	12 ± 2 ^c	1.0	2.0
G-CuONPs	13 ± 3 ^b	1.0	2.0	16 ± 2 ^b	1.0	2.0
Ampicillin	32 ± 3 ^a	16.1	16.1	37 ± 2 ^a	16.1	16.1

*MIC and MBC of *C. sappan* extract, copper sulfate, and G-CuONPs are in mg/mL, but that of ampicillin are in µg/mL. Lowercase letters indicate significantly different ($P < 0.05$) for inhibition zone between samples for each strain.

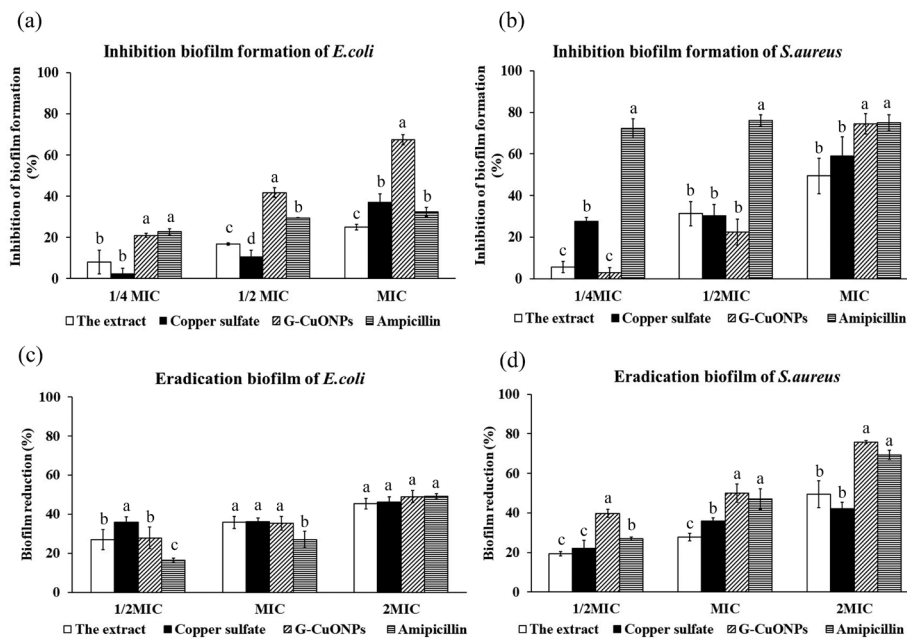


Figure 7. Inhibitory effects of the samples on biofilm forming of *E. coli* (a) and *S. aureus* (b), and effects of the samples on eradication of the formed biofilms of *E. coli* (c) and *S. aureus* (d). Lowercase letters are significantly different ($P < 0.05$) for each effect in the same concentration of the samples.

antibacterial activity as shown in Table 2. The inhibition zone against the test pathogenic bacteria of *C. sappan* extract was less than that of copper sulfate and G-CuONPs. The inhibition zone of copper sulfate against *E. coli* was wider than that against *S. aureus* whereas the inhibition zone of G-CuONPs against *E. coli* was less than that against *S. aureus*. The MIC and MBC values for all test samples were in the range of 1.0-2.0 mg/mL against both pathogenic bacteria.

The biofilm forming inhibition of the samples against *E. coli* and *S. aureus* is a dose dependent manner as shown in Figure 7 (a) and 7 (b), respectively. Treatment with 1/4 MIC, 1/2 MIC and MIC of the samples, *C. sappan* extract inhibited *E. coli* biofilm formation by 8.10 ± 5.77 , 16.76 ± 0.65 and $24.89 \pm 1.35\%$, respectively, whereas the inhibition of *S. aureus* film formation was 5.60 ± 2.62 , 31.25 ± 5.83 and $49.37 \pm 8.48\%$, respectively. Copper sulfate inhibited biofilm formation of *E. coli* by 13.93 ± 8.11 , 36.01 ± 2.57 and $36.10 \pm 2.07\%$ and that of *S. aureus* by 2.36 ± 2.68 , 10.50 ± 3.37 and

$37.13 \pm 4.09\%$. G-CuONPs inhibited biofilm formation of *E. coli* by 20.96 ± 0.87 , 41.68 ± 2.34 and $67.41 \pm 2.39\%$ and that of *S. aureus* by 2.95 ± 2.45 , 22.28 ± 6.21 , 60.16 ± 4.57 and $74.55 \pm 4.90\%$, respectively. At MIC, the biofilm forming inhibition against *E. coli* of G-CuONPs was $67.41 \pm 2.39\%$, significantly higher than that of ampicillin ($29.46 \pm 0.17\%$). The effective inhibition of *S. aureus* biofilm forming of G-CuONPs was $74.55 \pm 4.90\%$, similar to that of ampicillin ($75.01 \pm 3.80\%$). The eradication effects on *E. coli* and *S. aureus* biofilms of the samples at concentrations of 1/2MIC, MIC and 2MIC are shown in Figure 7 (c) and (d), respectively. It was found that treatment with *C. sappan* extract at the three concentrations could eradicate *E. coli* biofilm by 27.08 ± 5.13 , 35.76 ± 3.07 and $45.36 \pm 2.79\%$, respectively, whereas the eradication effect of *S. aureus* biofilms was 19.33 ± 1.19 , 27.72 ± 1.93 and $49.47 \pm 6.79\%$, respectively. In the presence of copper sulfate, there was 36.01 ± 2.57 , 36.10 ± 2.07 and $46.13 \pm 2.78\%$ reduction of the formed *E. coli* biofilms and

21.97 ± 4.17, 35.91 ± 1.61 and 42.16 ± 3.12% reduction of the formed *S. aureus* biofilms, respectively. G-CuONPs eradicated *E. coli* biofilms by 27.85 ± 5.61, 35.33 ± 3.48 and 48.90 ± 3.12% whereas their eradication of *S. aureus* biofilms was 39.75 ± 2.07, 49.99 ± 4.70 and 75.83 ± 0.89%, respectively. At the highest test concentration (2 MIC), G-CuONP showed no significant difference with ampicillin in eliminating *S. aureus* biofilm.

4. Discussion

Plants have a high ability to synthesize an almost unlimited number of substances. Among them, there are many substances that have medicinal potential in promoting health and treating disease. The heartwood of *C. sappan* has been historically used by local people as a traditional medicine and a coloring agent in food, cosmetics, and garments. In the current study, a preliminary phytochemical screening test revealed that the aqueous extract of *C. sappan* contained tannins, saponins and flavonoids but no terpenoids. Tannins are water-soluble polyphenols and are well documented in possessing antimicrobial, antimutagenic, and anticarcinogenic activities (29). Saponins are traditionally used as natural detergents and have a wide range in biological activities due to their amphiphilic structure (30). Flavonoids are a group of phytochemical compounds having polyphenolic structure with high medicinal benefits including anticancer, antioxidant, anti-inflammatory, and antiviral properties (31). These phenolic compounds possess hydroxyl and carboxylic groups, which allow to act as a reducing agent (32). Therefore, it is supposed that these bioactive phenolic compounds in *C. sappan* extracts facilitate the formation of CuONPs.

Characterization of the synthesized CuONPs is to confirm the complete nanoparticle formation. The absorption spectrum confirmed the formation of CuONPs due to the same surface plasmon resonance in the previous reports, which appears in the range of 200-300 nm (33,34). The FTIR spectra of G-CuONPs showed the peaks which correspond to functional groups of the extract. This indicates that the synthesized G-CuONPs absorbed some phytochemicals of the extract onto their surface. It was found that biological molecules of the extract could be responsible for formation and stabilization of synthesized G-CuONPs

Particle analysis by SEM and DLS demonstrates that the synthesized G-CuONPs have a spherical shape and size in the nano range with a narrow size distribution. Interestingly, the obtained nanoparticles are less aggregation with high negative zeta potential. The zeta potential values of nanoparticles approximately within +30 mV and -30 mV are sufficient to preserve strong repulsion between each particle and prevent aggregation of the nanoparticles (35). The high negative zeta potential of the obtained G-CuONPs is due to their surface

absorbing some negatively charged bioactive phenolic compounds of *C. sappan* extract which is confirmed by the FTIR results. The result of EDX confirms that the obtained CuONPs are composed of copper and oxygen atoms. The carbon signal in the EDX pattern might be derived from the compounds in the extract. From XRD analysis, the result confirmed the crystalline structure of the obtained CuONPs which are consistent with previous studies (34). The results of these characterizations confirm the success in synthesizing G-CuONPs from *C. sappan*.

The action of *C. sappan* extract is not only related to reducing activity in the synthesis reaction and stabilization of G-CuONPs but also enhanced the antioxidant capacity of synthesized G-CuONPs. The ABTS and FRAP assays are standard tools for testing antioxidant activities of the samples (36,37). Two mechanisms of actions can be derived from these methods. ABTS can be used to measure scavenging activity while FRAP can measure the reducing activity related to electron transfer ability of the samples. The IC₅₀ and EC values reflect the potency for these mechanisms, respectively. In the current study, G-CuONPs synthesized from *C. sappan* extract revealed both the scavenging and reducing activities almost same potency as the extract.

Glycation is an endogenous reaction between proteins and reducing sugars that can produce to AGE (38). Accumulation of AGE can cause several severe diseases including diabetes-associated complications and amyloid based neurodegenerative diseases (39). Therefore, the antiglycation effect of the samples is essential for health promotion. The study of antiglycation activity can be performed using two different models: BSA-ribose and BSA-MGO models. In the BSA-ribose model, ribose and its oxidation products react with the proteins until the reaction ends and the final product is AGE. In the BSA-MGO model, MGO is a highly reactive α -dicarbonyl compound, which is generated by the auto-oxidation of glucose and a potent precursor of AGE (40). MGO formation and accumulation has been implicated in the pathogenesis of diabetes due to oxidative stress. This study focused on preventing protein glycation. Therefore, BSA-ribose and BSA-MGO models were utilized to evaluate the inhibitory effect of the samples in both early-stage (BSA-ribose) and middle stage (BSA-MGO) of glycation products. Our results revealed that G-CuONPs have different inhibitory effects in a concentration-dependent manner. G-CuONPs show the highest activity in the BSA-ribose model. Their scavenging activity may inhibit the formation of AGEs in the early stage. Moreover, G-CuONPs may bind with free amino groups (lysine and arginine) in amino acids, which are potential sites for glycation in addition to the N-terminal amino acid. They are the key sites to be attacked by glyating agents. Some studies supported the idea that metal nanoparticles such

as selenium, zinc oxide, and silver may prevent AGE formation by covering these sites (41–43). However, the exact mechanism behind the inhibitory effect of metal nanoparticles is not yet fully known. In the BSA-MGO model, aminoguanidine shows the highest inhibitory effect. However, aminoguanidine has been reported for kidney problems in a phase III clinical trial in type 1 diabetic patients. Our findings indicate that G-CuONPs act as potential antiglycation agents in a concentration-dependent manner, especially in BSA-ribose model. For antibacterial activity, G-CuONPs show antibacterial and antibiofilm activities against *S. aureus* (Gram positive) than *E. coli* (Gram negative). Copper ions have a higher affinity to bind with carboxyl and amine groups on the cell surface viability (44). It is considered that CuONPs were adsorbed onto the bacterial cell surface and could damage the cell membrane leading to an increase of cellular permeability and reduction of bacterial viability. In addition, it has been reported that copper can also damage nucleic acids of the cells (45). Our findings indicate that G-CuONPs possess higher antibacterial and antibiofilm activities against Gram-positive *S. aureus* than Gram-negative *E. coli*.

In conclusion, the current study reports that the successful synthesis of G-CuONPs using *C. sappan* extract as a reducing agent. The synthesis method used is a simple and ecofriendly green process. It is found that the bioactive phenolic compounds in *C. sappan* extract played a crucial key in the synthesis and properties of G-CuONPs. The resulting G-CuONPs possess several beneficial properties including antioxidant, antiglycation, and antibacterial activities. Thus, the synthesized G-CuONPs may be effectively utilized for medical and pharmaceutical applications.

Acknowledgements

We would like to thank the Center of Excellence in Pharmaceutical Nanotechnology, Faculty of Pharmacy, Chiang Mai University for facility support.

Funding: This work was supported by a grant from Thailand Research Fund through the Research and Researcher for Industry (RRi) Grant number PHD59I0076.

Conflict of Interest: The authors have no conflicts of interest to disclose.

References

- Halwani AA. Development of pharmaceutical nanomedicines: From the bench to the market. *Pharmaceutics*. 2022; 14:106.
- Couto C, Almeida A. Metallic nanoparticles in the food sector: A mini-review. *Foods*. 2022; 11:10-12.
- Chavali MS, Nikolova MP. Metal oxide nanoparticles and their applications in nanotechnology. *SN Appl Sci*. 2019; 1:607.
- Baig N, Kammakakam I, Falath W, Kammakakam I. Nanomaterials: A review of synthesis methods, properties, recent progress, and challenges. *Mater Adv*. 2021; 2:1821-1871.
- Manuja A, Kumar B, Kumar R, Chhabra D, Ghosh M, Manuja M, Manuja A, Brar B, Pal Y, Tripathi BN, Prasad M. Metal/metal oxide nanoparticles: Toxicity concerns associated with their physical state and remediation for biomedical applications. *Toxicol Rep*. 2021; 8:1970-1978.
- Grigore ME, Biscu ER, Holban AM, Gestal MC, Grumezescu AM. Methods of synthesis, properties and biomedical applications of CuO nanoparticles. *Pharmaceutics*. 2016; 9:75-88.
- Salem SS, Fouda A. Green synthesis of metallic nanoparticles and their prospective biotechnological applications: An overview. *Biol Trace Elem Res*. 2011; 199:344-370.
- Iravani S. Green synthesis of metal nanoparticles using plants. *Green Chem*. 2011; 13:2638-2650.
- Sarkar J, Chakraborty N, Chatterjee A, Bhattacharjee A. Green synthesized copper oxide nanoparticles ameliorate defence and antioxidant enzymes in *Lens culinaris*. *Nanomaterials*. 2020; 10:312.
- Singh P, Singh KRB, Singh J, Das SN, Singh RP. Tunable electrochemistry and efficient antibacterial activity of plant-mediated copper oxide nanoparticles synthesized by *Annona squamosa* seed extract for agricultural utility. *RSC Advanc*. 2021; 11:18050-18060.
- Sathiyavimal S, Durán-Lara EF, Vasantharaj S, Saravanan M, Sabour A, Alshiekheid M, Lan C, Nguyen T, Brindhadevi K, Pugazhendhi A. Green synthesis of copper oxide nanoparticles using *Abutilon indicum* leaves extract and their evaluation of antibacterial, anticancer in human A549 lung and MDA-MB-231 breast cancer cells. *Food Chem Toxicol*. 2022; 168:113330.
- Hu J, Yan X, Wang W, Wu H, Hua L, Du L. Antioxidant activity *in vitro* of three constituents from *Caesalpinia sappan* L. 2008; 13:474-479.
- Rajput MS, Nirmal NP, Nirmal SJ, Santivarangkna C. Bio-actives from *Caesalpinia sappan* L.: Recent advancements in phytochemistry and pharmacology. *South African J Bot*. 2022; 151:60-74.
- Suwan T, Wanachantararak P, Khongkhunthian S, Okonogi S. Antioxidant activity and potential of *Caesalpinia sappan* aqueous extract on synthesis of silver nanoparticles. *Drug Discov Ther*. 2018; 12:259-266.
- Sasarom M, Wanachantararak P, Chaijareenont P, Okonogi S. Biosynthesis of copper oxide nanoparticles using *Caesalpinia sappan* extract: *In vitro* evaluation of antifungal and antibiofilm activities against *Candida albicans*. 2023; 17:238-247.
- Kokate CK. Practical pharmacognosy. 4 th. New Delhi: Vallabh Prakashan; 2005. pp.7-111.
- Nantitanon W, Yotsawimonwat S, Okonogi S. Factors influencing antioxidant activities and total phenolic content of guava leaf extract. *LWT - Food Sci Technol*. 2010; 43:1095-1103.
- Okonogi S, Duangrat C, Anuchpreeda S, Tachakittirungrod S, Chowwanapoonpohn S. Comparison of antioxidant capacities and cytotoxicities of certain fruit peels. *Food Chem*. 2007; 103:839-846.
- Sadowska-Bartosz I, Galiniak S, Bartosz G. Kinetics of glycoxidation of bovine serum albumin by glucose, fructose and ribose and its prevention by food components.

- Molecules. 2014; 19:18828-18849.
20. Froidi G, Djeujo FM, Bulf N, Caparelli E, Ragazzi E. Comparative evaluation of the antiglycation and anti- α -glucosidase activities of baicalein, baicalin (baicalein 7-o-glucuronide) and the antidiabetic drug metformin. 2022; 14:2141.
 21. Peng X, Zheng Z, Cheng KW, Shan F, Ren GX, Chen F, Wang M. Inhibitory effect of mung bean extract and its constituents vitexin and isovitexin on the formation of advanced glycation endproducts. Food Chem. 2008; 106:475-481.
 22. Puttipan R, Wanachantararak P, Khongkhunthian S, Okonogi S. Effects of *Caesalpinia sappan* on pathogenic bacteria causing dental caries and gingivitis. Drug Discov Ther. 2017; 11:316-322.
 23. Phumat P, Khongkhunthian S, Wanachantararak P, Okonogi S. Comparative inhibitory effects of 4-allylpyrocatechol isolated from *Piper betle* on *Streptococcus intermedius*, *Streptococcus mutans*, and *Candida albicans*. Arch Oral Biol. 2020; 113:104690.
 24. Séro L, Sanguinet L, Blanchard P, Dang BT, Morel S, Richomme P, Séraphin D, Derbré S. Tuning a 96-well microtiter plate fluorescence-based assay to identify AGE inhibitors in crude plant extracts. Molecules. 2013; 18:14320-14339.
 25. Alrubaye A, Motovali-Bashi M, Miroliaei M. Rosmarinic acid inhibits DNA glycation and modulates the expression of Akt1 and Akt3 partially in the hippocampus of diabetic rats. Sci Rep. 2021; 11:20605.
 26. Schalkwijk CG, Stehouwer CDA. Methylglyoxal, a highly reactive dicarbonyl compound, in diabetes, its vascular complications, and other age-related diseases. Physiol Rev. 2020; 100:407-461.
 27. Chung KT, Wong TY, Wei CI, Huang YW, Lin Y. Tannins and human health: A review. Crit Rev Food Sci Nutr. 1998; 38:421-464.
 28. Juang YP, Liang PH. Biological and pharmacological effects of synthetic saponins. Molecules. 2020; 25:4974.
 29. Ullah A, Munir S, Badshah SL, Khan N, Ghani L, Poulson BG, Emwas AH, Jaremko M. Important flavonoids and their role as a therapeutic agent. Molecules. 2020; 25:5243.
 30. Marslin G, Siram K, Maqbool Q, Selvakesavan RK, Kruszka D, Kachlicki P, Franklin G. Secondary metabolites in the green synthesis of metallic nanoparticles. Materials (Basel). 2018; 11:940.
 31. Abboud Y, Saffaj T, Chagraoui A, Bouari AEI, Brouzi K, Tanane O, Ihssane B. Biosynthesis, characterization and antimicrobial activity of copper oxide nanoparticles (CONPs) produced using brown alga extract (*Bifurcaria bifurcata*). Appl Nanosci. 2014; 4:571-576.
 32. Kumar B, Smita K, Cumbal L, Debut A, Angulo Y. Biofabrication of copper oxide nanoparticles using Andean blackberry (*Rubus glaucus* Benth.) fruit and leaf. J Saudi Chem Soc. 2017; 21:475-480.
 33. Nirmal NP, Rajput MS, Prasad RGSV, Ahmad M. Brazilin from *Caesalpinia sappan* heartwood and its pharmacological activities: A review. Asian Pac J Trop Med. 2015; 8:421-430.
 34. Verma PR, Khan F. Green approach for biofabrication of CuO nanoparticles from *Prunus amygdalus* pericarp extract and characterization. Inorg Nano-Metal Chem. 2019; 49:69-74.
 35. Singare DS, Marella S, Gowthamrajan K, Kulkarni GT, Vooturi R, Rao PS. Optimization of formulation and process variable of nanosuspension: An industrial perspective. Int J Pharm. 2010; 402:213-220.
 36. Xiao F, Xu T, Lu B, Liu R. Guidelines for antioxidant assays for food components. Food Front. 2020; 1:60-69.
 37. Nantitanon W, Okonogi S. Comparison of antioxidant activity of compounds isolated from guava leaves and a stability study of the most active compound. Drug Discov Ther. 2012; 6:38-43.
 38. Iannuzzi C, Borriello M, Carafa V, Altucci L, Vitiello M, Balestrieri ML, Ricci G, Irace G, Sirangelo I. D-ribose-glycation of insulin prevents amyloid aggregation and produces cytotoxic adducts. Biochim Biophys Acta - Mol Basis Dis. 2016; 1862:93-104.
 39. Singh R, Barden A, Mori T, Beilin L. Advanced glycation end-products: A review. Diabetologia. 2001; 44:129-146.
 40. Singh VP, Bali A, Singh N, Jaggi AS. Advanced glycation end products and diabetic complications. Korean J Physiol Pharmacol. 2014; 18:1-14.
 41. Yu S, Zhang W, Liu W, Zhu W, Guo R, Wang Y, Zhang D, Wang J. The inhibitory effect of selenium nanoparticles on protein glycation *in vitro*. Nanotechnology. 2015; 26:145703.
 42. Kumar D, Bhatkalkar SG, Sachar S, Ali A. Studies on the antiglycating potential of zinc oxide nanoparticle and its interaction with BSA. J Biomol Struct Dyn. 2020; 39:6918-6925.
 43. Ashraf JM, Ansari MA, Khan HM, Alzohairy MA, Choi I. Green synthesis of silver nanoparticles and characterization of their inhibitory effects on AGEs formation using biophysical techniques. Sci Rep. 2016; 6:20414.
 44. Karlsson HL, Cronholm P, Hedberg Y, Tornberg M, Battice LD, Svedhem S, Wallinder IO. Cell membrane damage and protein interaction induced by copper containing nanoparticles-Importance of the metal release process. Toxicol. 2013; 313:59-69.
 45. Festa RA, Thiele DJ. Copper: An essential metal in biology copper in prokaryotes. Curr Biol. 2011; 21:877-883.

Received May 9, 2024; Revised June 20, 2024; Accepted June 22, 2024.

*Address correspondence to:

Siriporn Okonogi, Center of Excellence in Pharmaceutical Nanotechnology, Faculty of Pharmacy, Chiang Mai University, Chiang Mai 50200, Thailand.

E-mail: okng2000@gmail.com

Released online in J-STAGE as advance publication June 28, 2024.